THE NEOSSAT EXPERIENCE: 5 YEARS IN THE LIFE OF CANADA'S SPACE SURVEILLANCE TELESCOPE

V. Abbasi[1], S. Thorsteinson[2], D. Balam[3] , J. Rowe[4], D. Laurin[1], L. Scott[2], M. Doyon[1]

[1] *Canadian Space Agency, 6767 route de l'aeroport, St-Hubert, Quebec, J3Y 8Y9, Canada,*
viqar.abbasi@canada.ca, denis.laurin@canada.ca, michel.doyon@canada.ca
[2] *Defence Research and Development Canada, 3701 Carling Ave, Ottawa, K2K 2Y7 Canada,*
stefan.thorsteinson@drdc-rddc.gc.ca, robert.scott@drdc-rddc.gc.ca
[3] *Spaceguard Consulting, 6421 Anndon Place, Victoria, British Columbia, V8Z 5R9, Canada,*
spaceguardc@shaw.ca
[4] *Bishops University, 2600 College St, Sherbrooke, Quebec J1M 1Z7, Canada, jrowe@ubishops.ca*

ABSTRACT

Canada's Near-Earth Object Surveillance Satellite (NEOSSat) is the world's first space telescope for dual-mode space surveillance of near-Earth asteroids/comets and man-made resident space objects orbiting the Earth. Launched in February 2013 and jointly funded by the Canadian Space Agency (CSA) and Defence Research & Development Canada (DRDC) as a low-cost technology demonstration microsatellite with minimal redundancy, NEOSSat operations continue into its fifth year on-orbit.

This paper summarizes the evolution, accomplishments and challenges that NEOSSat faced over its five years on-orbit, including a highly innovative software-based recovery of the satellite from two major hardware failures that crippled the attitude control system for over a year. The lessons learned and ongoing operational experience from this mission can be invaluable for future space-based missions performing tracking and characterization of near-Earth objects and resident space objects in high Earth orbit and even low Earth orbit.

1. MISSION BACKGROUND

In the past decade there has been a concerted effort to establish an international asteroid early warning system, beginning with a resolution prepared at the 2012 general assembly of the International Astronomical Union (IAU) [1]. In essence, it is stated that there is now ample evidence that the probability of catastrophic impacts of Near-Earth Objects (NEOs) with Earth is not negligible, and for humankind in particular, that appropriate actions are being developed to avoid such catastrophes.

The NEOSSat project supports NEO survey and asteroid science [2]. Furthermore, DRDC, in partnership with the CSA, developed NEOSSat to perform the High Earth Orbit Space Surveillance (HEOSS) Space Situational Awareness (SSA) technology demonstration mission. NEOSSat's HEOSS mission focuses on space-based characterization of deep-space, Resident Space Objects (RSOs) in geosynchronous (GEO) orbit from an observer orbiting in Low Earth Orbit (LEO). A LEO based space surveillance platform provides unique advantages for Canadian SSA operations. These include the ability to observe uninterrupted in the day-night cycle, in absence of terrestrial weather, and visibility to the entire geosynchronous belt, outside of Canadian geographic longitudes.

The prime contractor for NEOSSat was Microsat Systems Canada Inc. (MSCI), a Canadian company with spaceflight heritage through the space telescope Microvariability and Oscillations of STars (MOST) [3]. The company continues to provide sustaining engineering support to the operations team. The satellite is operated from CSA's multi-mission Satellite Operations Centre, also located in St-Hubert, Canada, with payload tasking support from DRDC Ottawa.

2. SATELLITE DESIGN

NEOSSat's primary payload is a 15-cm aperture Maksutov optical telescope with 0.85 degree field of view, featuring two E2V 1024x1024 charge-coupled devices (CCD) and associated read-out electronics providing 3 arcseconds/pixel resolution. One CCD unit is used for science imaging and the second is used for the specialized narrow-field star tracker sharing the optical boresight and field of view. This custom star tracker enables high-precision fine pointing at celestial targets and precise tracking of fast moving objects.
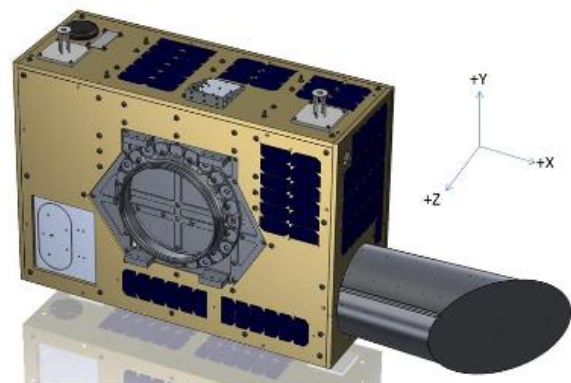

Figure 1 NEOSSat drawing with body axes definition

NEOSSat's large baffle allows the telescope to make observations near the Sun, down to 45 degrees solar elongation, a region difficult to image with ground telescopes. During "eclipse season", when the satellite's orbital plane is aligned such that the Earth obscures the Sun during the orbit, enabling imaging at much smaller solar elongations due to the Earth serving as a baffle.

The attitude determination and control system includes one three-axis magnetometer, coarse sun sensing derived from the solar panel output on each face, four reaction wheels with integrated rate sensors (X, Y, Z, Skew), three torque rods (X, Y, Z), and the custom narrow-field star tracker using the telescope boresight. Two GPS receivers are also included for orbit determination, one of the +Y size and another on the –Y face (Fig. 1). The magnetometer and coarse sun sensor are used for coarse attitude determination, whose solution is then used to seed the star tracker for fine attitude determination and the precise Fine Point control mode, which is maintained using the star tracker, rate sensors and reaction wheels. Torque rods are used for desaturation of the reaction wheels, dumping the excess momentum that builds up as a result of the control loop responding to disturbance torques. Altogether, the microsatellite weighs 73 kg.

The NEOSSat architecture is based upon and improves upon the architecture of the successful MOST space telescope. It is the first implementation of a generic multi-mission microsatellite bus that can be readily adapted to new mission types.
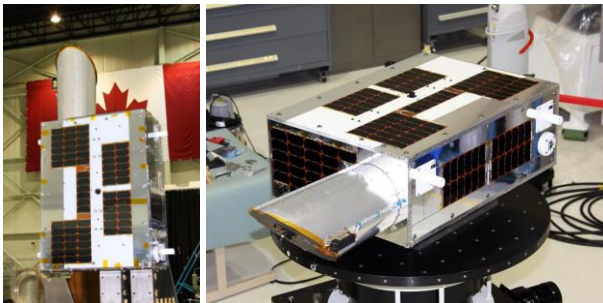

Figure 2 NEOSSat during integration testing

3. EARLY OPERATIONS

3.1. Launch and Early Operations

NEOSSat was launched on February 25, 2013, on the Indian Space Research (ISRO) Polar Satellite Launch Vehicle (PSLV) Flight C-20, as one of six secondary payloads. Another secondary payload on the same launch was the Canadian space surveillance satellite Sapphire (Fig. 2), owned and operated by the Canada's Department of National Defence (DND) as a dedicated contributing sensor to the United States Space Surveillance Network (SSN). The primary payload of PLSV C-20 was the Indian and French remote sensing satellite SARAL, which controlled the launch schedule.

With hardware integration and testing taking priority in the months preceding launch, NEOSSat was shipped to the launch site with a minimal suite of flight software onboard, with sufficient communications functionality to upload new software on-orbit. The remaining flight software for imaging with fine pointing attitude control would be completed and uploaded in commissioning.

Figure 3 NEOSSat & Sapphire launch configuration

Figure 4 PSLV C-20 launch (Credit: ISRO)

3.2. Satellite Commissioning

The successful launch placed all satellites in 780 km sun-synchronous orbits. Early NEOSSat passes were supported by Canadian S-band ground stations in St-Hubert/Canada and Saskatoon/Canada as well as German S-band ground stations in Walheim/Germany and O'Higgins/Antarctica, operated by the DLR. Later, NEOSSat was also supported by Canada's new ground station in Inuvik/Canada and Gatineau/Canada.

Although communications with NEOSSat were robust and reliable, flight software updates were needed before all-sky fine pointing could be reliably achieved. The co-located payload/star-tracker optical design on NEOSSat required significant enhancement compared to its predecessor MOST, where star tracker parameters would be configured on the ground and uploaded to the satellite

for a given science target used for months. By contrast, NEOSSat required rapid autonomous all-sky acquisition for both its missions. While commercial star trackers typically have fields of view in the range of 8 to 35 degrees and operate mostly with bright stars, NEOSSat's boresight-aligned star tracker operates with a miniscule 0.8 degrees field of view, working autonomously with an onboard star catalog featuring 2 million guide stars down to visual magnitude 14. These features allow NEOSSat to achieve a high degree of pointing accuracy, but several software iterations were required to make the system operational, addressing issues such as optimal lit pixel lists and star catalog management and elimination of false positives under a variety of in-flight conditions. Ultimately, reliable all-sky star tracker acquisition and fine pointing was achieved, typically providing better than one arcsecond stability in Fine Point mode as well as maintaining star tracker custody during fine slews to enable highly accurate tracking of fast-moving objects.

Another significant effort during commissioning was related to CCD imager, where interference from the satellite electronics were found to be contributing noise on the CCD. These were addressed in two ways [4]. First, the CCD readout electronics flight software was updated with new features to synchronize the operations of the science and star tracker CCD to eliminate one source of interference. Second, science images were tasked to include an overscan region that was later analysed automatically in the ground image processing software using Fourier transforms to identify the major interference frequencies and to produce clean images by subtracting those noise contributions.
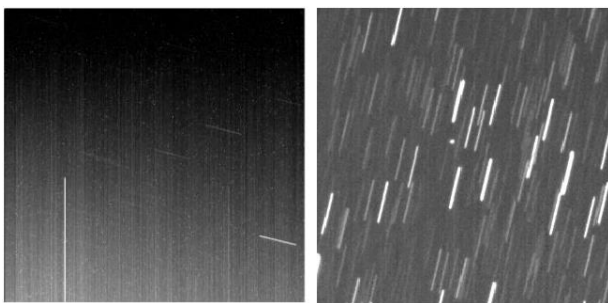

Figure 5 NEOSSat early ray imagery (left) and a cleaned image of featuring asteroid TC-04

With these flight and ground software upgrades, NEOSSat was ready to perform its science activities.

3.3. Near-Earth Object Survey Operations

Currently, we know of more than 19,000 near-Earth asteroids (NEAs) larger than 50 m and more than 100 near-Earth comets (NEC), with many more NEOs being discovered at a prodigious rate, as new and larger instruments (PanSTARRS, LSST) actively survey the sky. Most of the largest, potentially hazardous objects larger than 1 km diameter are now known, but there

remains a residual impact risk from the remaining unknown ~ 10% and sporadic long-period comets [5].

A significant portion of the undiscovered objects will likely be of interior orbit class (Aten, Atira); currently there are ~1500 known interior objects. Statistics suggest that there are about 10 times more 100m diameter objects in Earth-crossing orbits than the larger population of objects. This would imply, as a coarse estimate, that there could be as many as 10,000 objects in interior orbits larger that 100m in diameter.

The utilization plan for NEOSSat was for 50% time-sharing between space surveillance activities for DRDC and NEO survey/follow-up for CSA, focused on the interior orbit class. The planned survey cadence was 288 images/day, based on 24 images/orbit and 12 orbits/day, at 100s-exposure per image.

NEOSSat's slew and settle capabilities supported the required six 100s-exposure images per quarter-orbit, but many orbits were affected by the South Atlantic Anomaly (SAA), a region where charged particles would introduce noise into the CCD and render images scientifically unusable, as shown in Fig. 6.
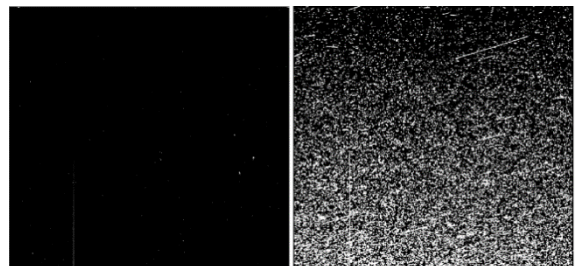

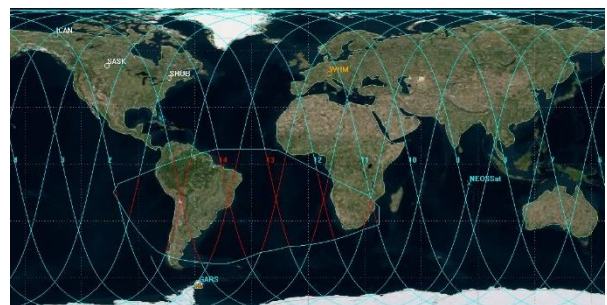*Figure 6 Two 1 second exposure dark frames taken outside the SAA (left) and over the SAA (right).*

Figure 7 SAA affects portions of 11 of 14 daily orbits, either on the ascending or descending node. Only time outside of SAA is suitable for NEO survey imaging.

Another complication was that NEOSSat lacks active temperature control and that the instrument's optical focus is only optimal within a specific temperature range. The operational workaround was to insert "cooling" periods, where the satellite's orientation was controlled relative to the Sun. These thermal stabilization periods (scheduled during orbits affected by SAA) improved the

telescope's optical focus before imaging, reducing the limiting magnitude achieved for 100-second exposures.

With appropriate planning and ground processing (including dark subtraction) to minimize image noise, the science team characterized NEOSSat's limiting magnitude at ~19 for 100s exposures under best-case conditions. Astrometric observations of known NEOs – including 405Thia, 194Pronke, 2006AD and Comet 249P (Fig. 8), were submitted to the IAU Minor Planet Center and NEOSSat was assigned Observatory Code C53.
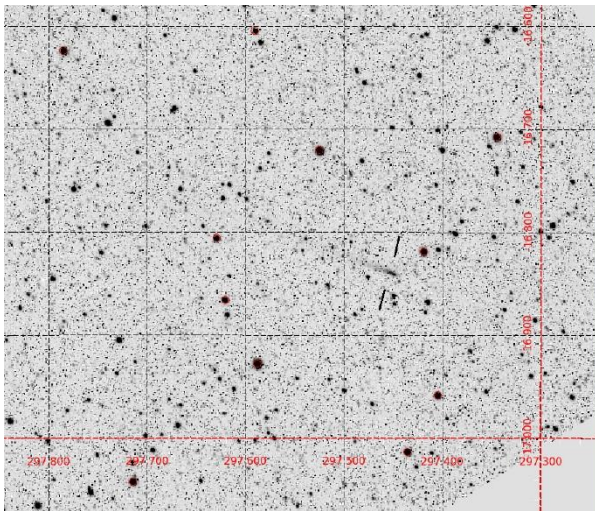

Figure *8 Comet 249P, displayed on equatorial grid with Tycho-2 catalogue stars marked in red.*

3.4.   Space Surveillance Activities

DRDC Ottawa tasks NEOSSat to track high Earth orbit RSOs of SSA research interest under the High Earth Orbit Space Surveillance (HEOSS) project. The HEOSS project focuses on tracking RSOs of interest, mainly consisting of operational Canadian geostationary assets. Also observed are GEO events of interest such as tracking through orbital re-positioning [6] and satellite anomaly characterization and recovery.

HEOSS utilizes NEOSSat's highly accurate fine slewing capabilities to image RSOs in Track Rate Mode (TRM) where NEOSSat is slewed to match the apparent motion of an RSO, which results in streaked stars and a point source RSO. NEOSSat's design requirements called for arcsecond level stability at slew rates up to 60 arcseconds/s. This requirement was chosen as rates to objects in GEO from a sun-synchronous orbit are all below this value. After commissioning NEOSSat demonstrated the ability to reliably perform fine slews at rates up to 90 arcseconds/s, enabling tracking at ranges significantly below GEO.

TRM imagery has the chief advantage that it maximizes the signal-to noise ratio of RSO signatures on the detector, but requires a-priori trajectory information of the target object. Since the telescope follows the RSO

during imaging, signal accumulates in a smaller area on the CCD relative to the more thinly distributed signal in RSO streaks resulting from imagery in Fine Point. Higher signal-to-noise ratio (SNR) leads to more accurate RSO position determination, as well as better estimate of the RSO photometric brightness.

To ensure spacecraft health, respect attitude control system limitations and ensure RSO visibility, NEOSSat must adhere to several constraints during HEOSS operations. The primary constraints applied during NEOSSat tracking are [7]:

NEOSSat Constraints

- NEOSSat +X direction of the Science detector is aligned toward the target RSO
- NEOSSat -Z solar panel is constrained Sunward to maintain power and thermal constraints
- Instrument radiator (+Z) points (preferentially) toward deep space
- NEOSSat is outside of the South Atlantic Anomaly during fine acquisition slew phase

Line-of-Sight Constraints

- RSO-centric solar phase angle is less than 135 degrees (outside of eclipse)
- Angular rate of the RSO relative to NEOSSat is < 90 arcseconds/second
- Grazing angle of RSO above the Earth limb is greater than > 10 degrees
- Lunar and planetary exclusion angles are >4 degrees

NEOSSat's geocentric position during metric observations is calculated with data from its dual Novatel OEMV1G GPS receivers. Simultaneously, this GPS receiver steers the onboard payload clock ensuring millisecond timing. GPS data is post-processed on the ground producing orbit ephemerides accurate to 2 meters (3-sigma), more than sufficient for metric measurements of deep space objects. A summary of NEOSSat's metric and photometric accuracy calibration and performance is available in [8].

Due to the non-linear motion of RSOs with respect to NEOSSat, and in order to limit the elongation of background stars required for astrometry, imagery acquired for HEOSS is of short (< 10s) exposure duration. NEOSSat acquires imagery at a rate of one full frame every 65 seconds in 1x1 binning and one frame every 20 seconds in 2x2 binning. This slow rate was a requirement of the NEO mission to allow CCD readout of faint signals near the image floor.

The HEOSS mission was well underway shortly after commissioning ended, providing exploitable SSA imagery from 2014 onwards.
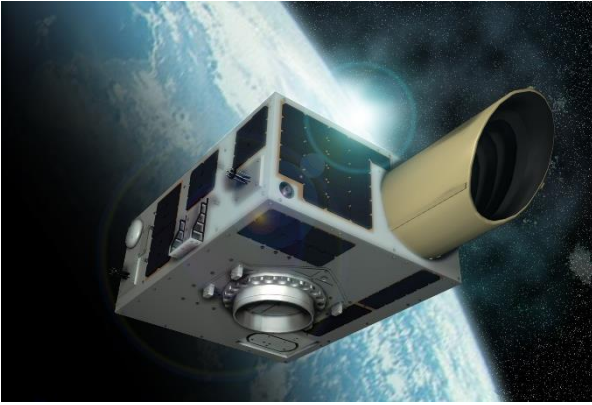
Figure 9 Artist's rendition of NEOSSat on-orbit

4. TWO MAJOR FAILURES & RECOVERY

4.1. Magnetometer Failure

Unfortunately, NEOSSat's scientific imaging came to an abrupt halt in early 2016 when the satellite's magnetometer suffered a permanent failure, resulting in noisy and unreliable measurements of the Earth's magnetic field. The failure is attributed to the harsh effects of the space environment, charged particles which routinely disrupt satellite electronics. Without the magnetometer, NEOSSat's attitude determination software could not solve for the coarse attitude solution required to transition to the fine attitude determination and control. The satellite remained a tumbling state, still communicating with the ground during passes, but completely inoperable for any science.

4.2. Maintaining Satellite's Health and Safety

The first priority was to manage the thermal state of the vehicle to ensure that the batteries would not overheat. Through satellite telemetry, the operations team monitored the system temperatures, angular momentum and tumble characteristics to maintain satellite health and safety. The objective was to ensure that the +Z face (side with the batteries) stayed away from the Sun. With no attitude control mode available, the operations team initially directly commanded the reaction wheels to change the direction of the angular momentum whenever the satellite was in a situation that the tumble maintained a major axis spin with the +Z consistently facing the Sun.

Maintaining the desired Sun vector was facilitated with the implementation of a flight software update providing a new Sun Point control mode. This mode used the only remaining functional coarse attitude sensor – the Sun sensor – to orient the vehicle relative to the Sun while minimizing the body rates. In this mode, the team could arrest NEOSSat's tumble to a greater extent, although a degree of freedom remained around the Sun vector.

While supporting spacecraft health, the Sun Point mode also allowed the team operations to open the shutter and take short exposure images that would serve as attitude truth to support the development of a new 3-axis attitude determination scheme for NEOSSat that did not depend on the failed magnetometer.

4.3. Attitude Determination Recovery

Many options were considered to recover NEOSSat attitude determination [9]. Ultimately, the team agreed to use the onboard GPS units – normally intended for orbit determination – as an attitude sensor, to be used in conjunction with the Sun sensor to provide three-axis attitude determination.

The new GPS-based attitude determination algorithm [10] makes use of the reported inertial positions of all GPS space vehicles contributing to the GPS solution as well as the elevation angle determined by the signal-to-noise ratio for each of these vehicles. Combining this information with the known and fixed configuration of the GPS receivers mounted on the satellite body, the new algorithm continually estimates the direction of the GPS receiver boresight. This GPS boresight vector estimate is coupled with the Sun vector estimate from the coarse sun sensor, providing the attitude determination software with two independent inertial orientation as required to solve for a full three-axis satellite inertial orientation.

Using an incremental and iterative approach, the flight software implementation of this innovative new attitude determination implementation was successful. The GPS attitude sensor and sun sensor are now the satellite's primary coarse attitude determination sensors, providing sufficient accuracy to enable transition to fine attitude determination with the star tracker, thereby fully recovering NEOSSat's ability to reliably achieve Fine Point at arbitrary user targets.

4.4. Torque Rod Controller Failure

Sadly, while the GPS attitude sensor was still in development, a second major anomaly crippled another key component of attitude control. The microcontroller used to communicate with the torque rods stopped communicating following a single-event upset, disabling the torque rods permanently and leaving no on-board actuator to dump the excess satellite momentum. Consequently, momentum would build up in the reaction wheels as the attitude control loop responded to disturbance torques increasing overall satellite momentum and eventually saturating the reaction wheels when they could no longer absorb any more momentum.

The strongest disturbance torque affecting attitude control was the satellite's own residual dipole, which remained present on-orbit despite design efforts to minimize it. The residual dipole was strong enough that without torque rods to dump the excess momentum, the reaction wheels could saturate in a matter of hours, depending on the target attitude. A new desaturation

strategy was needed if NEOSSat was to once again become a viable and productive satellite platform.

4.5. Attitude Control Recovery

To resolve the desaturation problem, the team developed an innovative new control mode which uses the satellite's own residual dipole to perform desaturation [9]. The new Dipole Desaturation control mode would make use of the now-recovered attitude determination system to optimize the satellite's pointing relative to the Earth's magnetic field, such that the residual dipole torque provides a net reduction in the satellite's total angular momentum. The desired desaturation target vector is continually updated throughout the satellite's orbit (to keep pace with the changing magnetic field) and the closed-loop control system attempts to maintain proximity to this ideal desaturation target vector at all times. Given that there are several optimal desaturation vectors at any given time (on the plane orthogonal to the magnetic field vector), another constraint is used to define a unique desaturation target vector. The best choice for a second constraint was to specify the desired sun vector in the body frame, as this could be used to maintain spacecraft thermal health and safety. Therefore, the control target in Dipole Desaturation mode is a continually-updated target formed by considering the satellite orientation relative to both the Earth's magnetic field and the Sun. In the inertial frame, the satellite is tumbling, but the tumble is actually tightly controlled using the coarse attitude sensors in an innovative closed-loop control system that actively dumps momentum and maintains satellite temperatures.

Dipole desaturation has proven effective and reliable, enabling a return to mission activities without functional torque rods. Fig. 10 demonstrates the momentum dumping performance from a fully saturated state. Once excess momentum is dumped, the system regains the control authority to perform the pointing tasks for scientific imaging. Momentum build-up does occur during controlled pointing for science, but science targets are not optimized for momentum build-up while the desaturation target is optimized for momentum dumping. As a result, the majority of the satellite's time can be devoted to scientific imaging.

Figure 10 Flight telemetry data showing momentum dumping in NEOSSat's Dipole Desaturation mode. Hyper-saturation is avoided operationally, ensuring rapid desaturation (~ 1 orbit) during routine operations

With no failures affecting the star tracker, rate sensors or reaction wheels, NEOSSat's Fine Point performance remains as robust as it was pre-failure. The fact that desaturation is no longer done in parallel by the torque rods but is instead performed routinely via the new dedicated control mode between science activities has resulted in a reduction in the duty cycle available for science, but no degradation in the attitude control performance itself.

4.6. New Open Data Initiative

Although the satellite was recovered and back to pre-failure performance, the extended outage and modified duty cycle to accommodate desaturation drove concerns about the feasibility of the original NEO survey plan and led to a new approach towards space astronomy tasking and data processing.

Post-recovery, CSA is supporting the Canadian government's Open Government initiative, making the astronomical images from NEOSSat available via its open data platform [11] and developing a more diversified scientific user base. As a result, NEOSSat is now supporting astronomy imaging activities beyond the original mission plan focussed on the NEO survey. In addition, led by DRDC, NEOSSat was used to further advance the state-of-the-art in space-based space surveillance, beyond the original mission goals.

5. ADVANCED SPACE SURVEILLANCE

5.1. Geostationary and High-Earth-Orbit Object Tracking

Due to the nature of a space based platform RSO tracking imagery acquired from NEOSSat requires specialized image processing algorithms. Fig. 11 shows a composite of NEOSSat imagery acquired during a single track on geostationary satellites Anik F2 and Wildblue-1. The satellites are identifiable as point sources on the imagery, however there are numerous sporadic point sources from energetic cosmic ray hits on all images. HEOSS' space surveillance imaging processing system [8] uses a matched filter to detect streaked background stars and a novel drift compensating stacking algorithm which simultaneously detects RSOs matching predicted motion rates and rejects noise artifacts from particle strikes. Space surveillance observations are then produced consisting of J2000 right ascension, declination and time.

NEOSSat's metric accuracy was assessed by observing GPS satellites and comparing these observations to precise GPS orbital ephemerides.
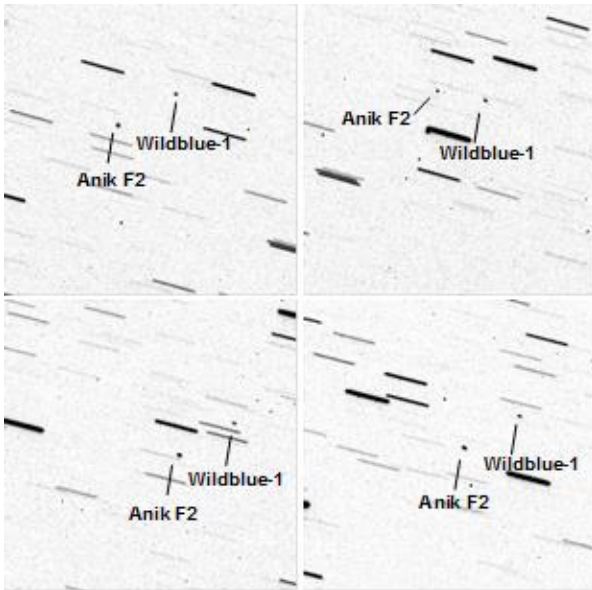
Figure 11 Sample HEOSS observations acquired on a single geostationary satellite track [7].

From the residuals from 414 GPS observations acquired post commissioning in from 15 Sep 2015 to 3 Feb 2016, the 1-sigma RMS metric accuracy of HEOSS observations was determined to be 2.76 arcseconds in 1x1 binning (Fig. 12).
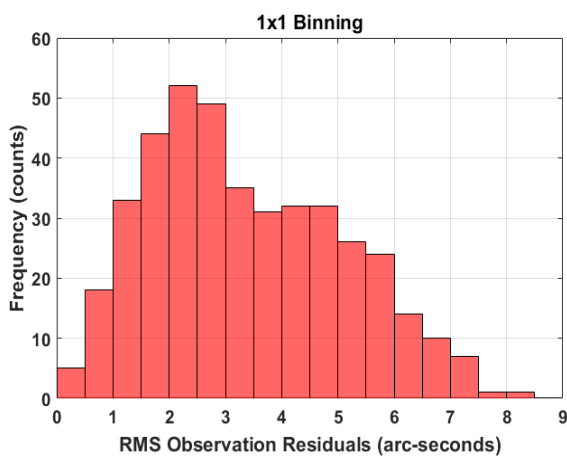

Figure 12 NEOSSat (HEOSS) mission RMS metric accuracy histogram [8].

The detected magnitudes of all NEOSSat GEO observations from 2016 to 2018 are shown in Fig. 13. The histogram is centred around magnitude 11.5 which corresponds to the peak brightness of the GEO population at minimum solar phase angle.

Using frame stacking, NEOSSat is sensitive to magnitude 16 with fully automated image processing. Under optimal conditions, slightly fainter objects can be detected but the system is largely insensitive to debris objects known to exist in GEO orbit fainter than magnitude 17.
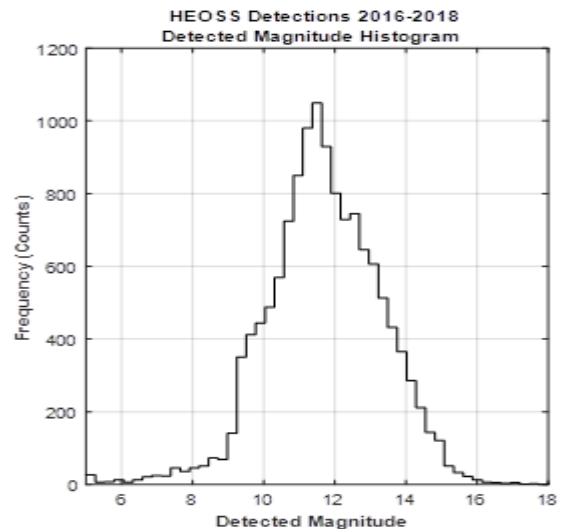

Figure 13 NEOSSat (HEOSS) mission photometric distribution of all detected GEO objects [7]

NEOSSat's stray light baffle allows for RSO imaging down 45 degrees of the Sun (or lower during eclipse conditions). This permits a persistent tracking of a GEO for three quarters of its 24 hour orbit, a level of custody not achieved with other sensors. Fig 14 shows the distribution of GEO observations from 2016-2018 with respect to their solar phase angle.
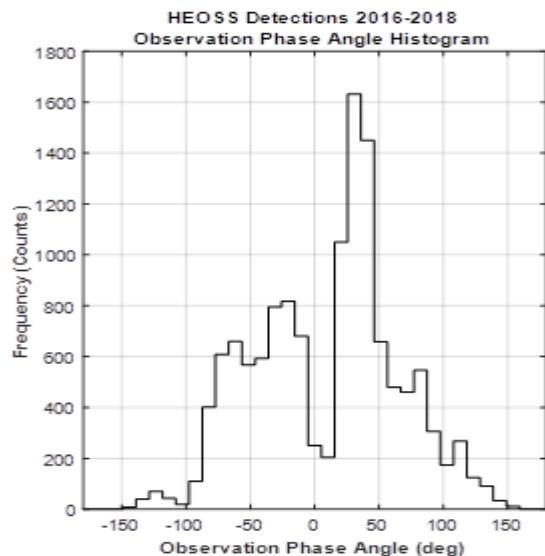

Figure 14. Distribution of the phase angles of the observations [7]

5.2. Low-Earth-Orbit Object Tracking

In the first five years of NEOSSat's mission, most HEOSS observations adhered to the SSA activities devised for the mission in 2009. Recently, improvements in ACS performance have enabled precision tracking of objects in LEO, in a variety of geometries. This includes tracking of orbital collision risks to NEOSSat itself (e.g.

conjuncting space objects), as well as instantaneous imagery of other conjunctions occurring in LEO. NEOSSat has shown remarkable fine slewing capabilities at rates up to 220 arcseconds/s. At these high rates the star tracker does not always contribute to the attitude control solution (when star streaks are too elongated and faint to be detected) but accurate fine slewing is achieved gyroscopically for short periods. At these high rates NEOSSat is able to observe a wide range of LEO objects for brief periods, and extended tracking of co-orbital objects for long periods. These new areas of SSA imaging are now discussed.

5.3. Conjunction Imaging

NEOSSat has begun observing objects undergoing low probability of collision conjunctions with itself. These are taken during the short period of visibility (~250s) from when a conjuncting object rises over the horizon and intersects NEOSSat's orbit at low range. Such trajectories exhibit motion described as "constant bearing – decreasing range", where the object has very small angular rates relative to NEOSSat where imagery can be collected in Fine Point before the Time of Closest Approach (TCA). Alternatively, if viewing geometry is more favourable, NEOSSat can also observe a secondary object's retreat from TCA.

CSA's Collision Risk Assessment & Mitigation System (CRAMS) [12] provides conjunction predictions for CSA satellites, including NEOSSat, based on Conjunction Data Messages (CDMs) made available to satellite operators by the United States Strategic Command (USSTRATCOM). In addition, forecasted conjunctions within 5 km of NEOSSat are available from the SOCRATES service provided by Celestrak [13]. These were used to select and plan conjunction viewing opportunities.

Figure 15 shows stacked images of the approach of Orbcomm FM-20 which made a close approach to NEOSSat on 29 Jun 2018. A total of seven observations were made, the first six in Fine Point mode and then NEOSSat was torqued to match the passing object's relative rate to allow one more image before it exceeded NEOSSat's slewing capability.

Several attempts were made to best match the sudden increase in relative angular rates between NEOSSat and a conjuncting object just before the TCA, while still keeping the object within NEOSSat's narrow field of view. In practice, only one or two 2x2 binned images could capture a conjuncting object in track-rate mode as it exited the initial set of Fine Point images, before the object's angular acceleration was beyond NEOSSat's slewing abilities.
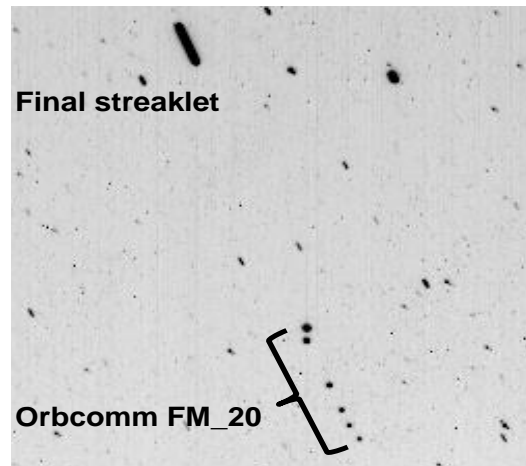

Figure 15 Stack of NEOSSat frames of Orbcomm FM-20 during its conjunction with NEOSSat.

When a secondary makes its closest approach to a satellite there is a rapid increase in angular rates causing it to streak in these images. Another example of stacked conjunction imagery is Fig. 16 which shows the close approach of Iridium 17 on 29 Jun 2018, excepting the imagery was acquired just past closest approach.
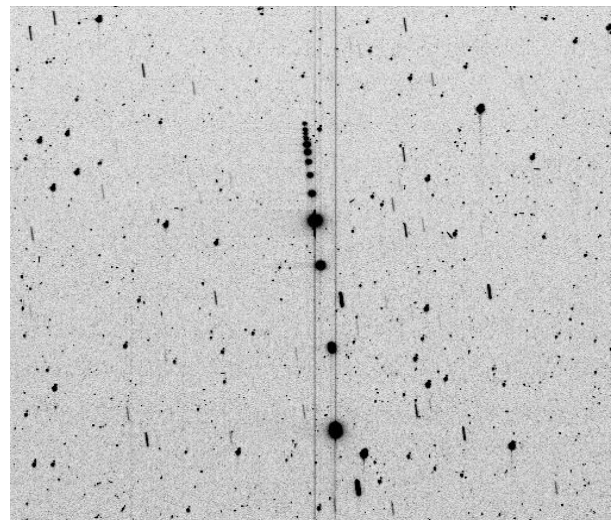

Figure 16 Iridium 17 stack showing the fade-out of the object retreating just after TCA

A similar incoming conjunction was imaged on 2 Aug 2018, as a piece of debris from COSMOS 2251 (NORAD ID #34023) made a close approach. This debris is a remnant from the infamous COSMOS 2251 collision with Iridium 33 in 2009.

The light curve for this debris is shown in Fig. 17. The debris varied in visual magnitude from 8.8 (160000 counts) at 500 km slant range to magnitude 14.5 (2300 counts) at 3000 km. This curve shows the characteristic $1/r2$ change in brightness one would expect from such an encounter. Tracks of self-conjuncting objects are phase-angle invariant as the observer line of sight is relatively

constant during the close approach, with Iridium 17 staying at a near constant 67.2 degrees solar phase angle throughout this encounter.
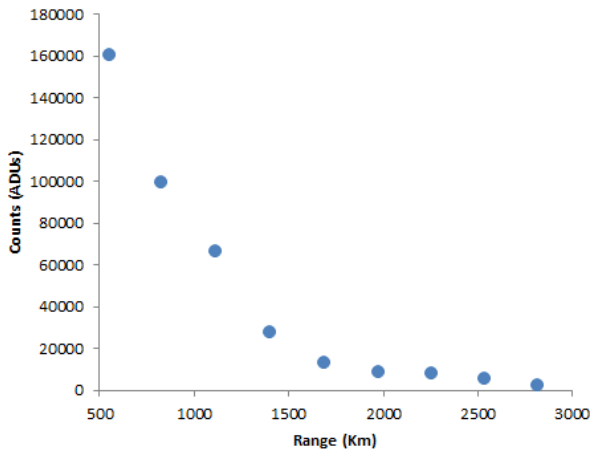

Figure 17 Light curve (counts) as COSMOS 2251 DEB (NORAD ID #34023) approaches NEOSSat.

Collecting a light curve during constant bearing – decreasing range conditions where the solar phase angle is fixed allows for inference of RSO properties such as tumbling state or size estimates.

5.4. Conjunction Re-analysis

On 10 Aug 2018, eight days after the conjunction from Fig. 16 another debris object from the COSMOS 2251 breakup (this time NORAD ID #33791) once again conjuncted with NEOSSat. Six observations were taken over a period of three minutes as the range between the two objects decreased from 2955 km down to 567 km, with the last observation approximately 38 seconds before the TCA. The relative orbit tracks just before the encounter are shown in Fig 17.
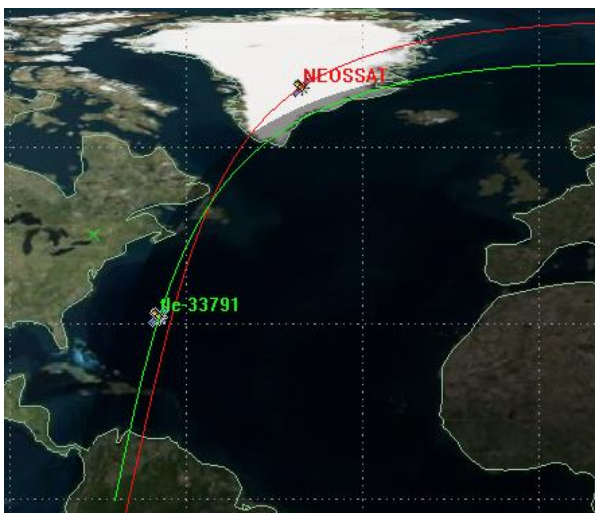

Figure 18 Relative orbits of NEOSSat and COSMOS 2251 DEB minutes before conjunction

The observations from this encounter were used to update the orbit state of the debris to see if any improvement in covariance, and thus possibly a better prediction of the miss distance at the TCA is possible. Fig 19 shows the results of orbit determination (using AGI's Orbit Determination ToolKit's extended Kalman filter [14]). The latest TLE before the encounter was used to seed the orbit, and the covariance left to inflate before the encounter. NEOSSat's observations provided a sharp decrease in the in-track component of the object's position uncertainty, despite the angles-only observations coming mainly in a head-on configuration.
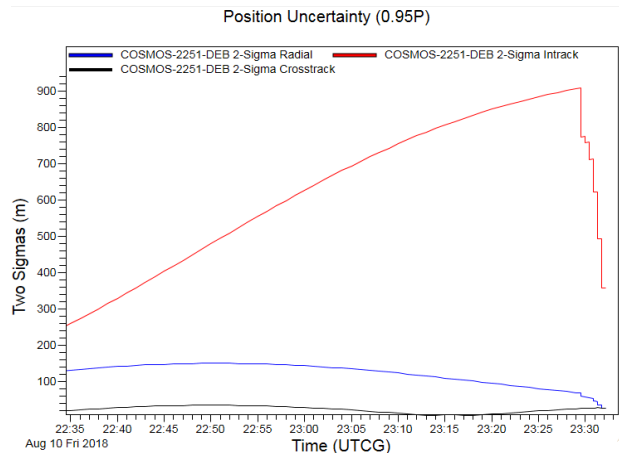

Figure 19 COSMOS-2251 DEB covariance improvement during conjunction imaging

This allowed for a slight improvement of the TCA computation and close approach distance. Table 1 shows the differences in predicted position of the object in the final frame of imagery, 38 seconds before the TCA. In addition to the TLE based conjunction prediction, a high precision orbit from the object's Special Perturbation (SP) vector ephemeris (made available from the US Joint Space Operations Centre). All three orbits were propagated to the image's observation time; the differences between the true position and the TLE prediction were on the order of 150 arcseconds, and 12 arcseconds for the SP vector ephemeris.

Table 1 – Image location (celestial coordinates) of COSMOS 2251 DEB #33791

Source	Right Ascension (HH MM SS.S)	Declination (DD MM SS.S)
TLE	15 28 45.8	-37 01 54.3
SP vector	15 28 54.5	-37 01 49.9
Updated orbit	15 28 54.1	-37 02 01.5

Fig. 20 shows an enhancement of the streaklet during the last image. The red dot near the centroid of the streak shows the object's Kalman filter solution position, with the SP vector in yellow and the TLE prediction in green.
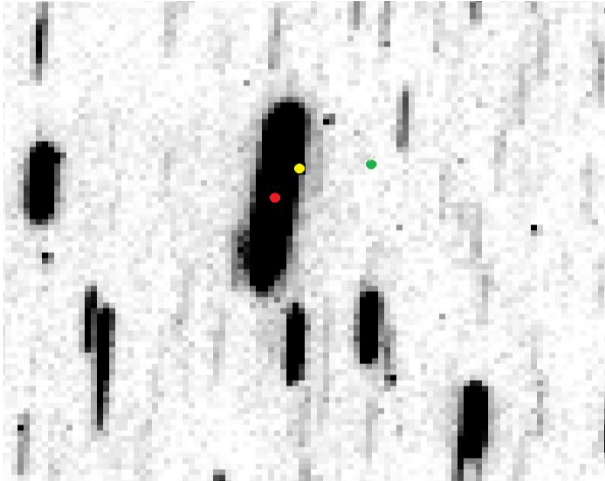

Figure 20 Enlarged streaklet of COSMOS-2251-DEB before conjunction. Updated orbit position (red), CDM prediction (yellow) and TLE prediction (green)

The predicted TCA and miss distance from the warning TLE and the Kalman filtered solution are shown below.

TCA from TLE:

```
Time (UTCG):          10 Aug 2018 23:32:50.147
Radial (km):          -3.327
In-Track (km):        0.239
Cross-Track (km):     2.280
Range (km):           4.040
```

Actual TCA:

```
Time (UTCG):          10 Aug 2018 23:32:50.177
Radial (km):          -3.261
In-Track (km):        0.275
Cross-Track (km):     2.555
Range (km):           4.152
```

The accuracy improvements from the Kalman filtered orbit are 30 ms in TCA and almost 150 m in miss distance. Such improvements suggest that a maneuverable satellite with similar imaging capabilities may be able to autonomously determine if an emergency maneuver is required ahead of the TCA. While this may be a stretch for LEO satellites the approach angles are similar in GEO where a hosted payload could detect conjuncting lower relative velocity debris not visible from the Earth in an effort to protect itself.

5.5. Medium Range High Value Asset Monitoring

The space surveillance satellite Sapphire is a High Value Asset (HVA) to the Canadian Forces. Co-orbital due to sharing the same launch as NEOSSat in 2013, it has unique in-track observing windows opportunities. Monitoring of this HVA in several geometries was investigated. This includes in-situ imaging of objects conjuncting with Sapphire at medium range (1000-5000 km). NEOSSat observed Sapphire conjuncting with two closely spaced Orbcomm satellites (34 and 35) on 6 July 2018 (Fig 21). The first at 17:26:15.3 UTC and the second at 20:47:05.4 UTC. Both images are one second exposures centered around the predicted TCA times.
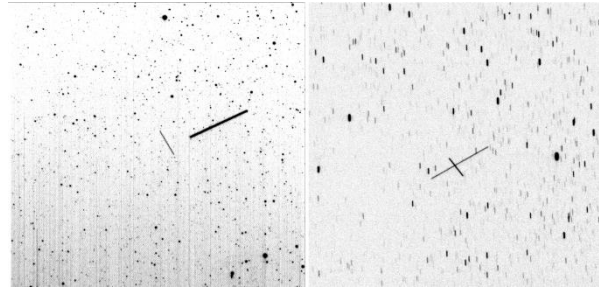

Figure 21 Sapphire (longer streak) conjuncting with Orbcomm 35 (left) and 34 (right)

The predicted distance of close approach for the Orbcomm 35 conjunction was 2.85 km and 2.12 km for Orbcomm 34 and it is clear from the images that the Orbcomm 34 conjunction was the nearer miss. The slant range from the Sapphire-Orbcomm 34 encounter to NEOSSat at the TCA was 2783 km, with an angles only separation between both objects being 61 arcseconds at the middle TCA the corresponds to a separation of 0.82 km while the radial separation relative to NEOSSat was 1.06 km.

Another interesting detail is that despite these two conjunctions being two orbits apart (3 hours, 21 minutes) NEOSSat is pointed at much the same starfield (about 0.25 degrees difference between the frames) due to the repeating nature of conjunctions in the sun-synchronous orbit regime.

5.6. Shared Orbit Monitoring

In the summer of 2018, imaging campaigns with the goal of maintaining orbit custody of objects sharing NEOSSat's orbit were conducted. These objects share the same orbit but at different true anomalies due to drag influences, which present specific imaging challenges. Provided the object was not obscured by the Earth (a situation which lasts about 3 months in the case of NEOSSat and Sapphire) NEOSSat could attempt to track it persistently in TRM. To slew down range at a target sharing your orbit is equivalent to keeping a nadir pointing orientation. At NEOSSat's altitude this requires a slew rate of 215 arcseconds/s. While this was outside of the star tracker's configured sensitivity limits, attempts to achieve these rates using purely gyroscopic slews without star tracker feedback proved successful.

On 13 Jul 2018 a series of such 215 arcseconds/s slews were performed while NEOSSat was approximately 3570 meters ahead of Sapphire in its orbit (Fig. 22).
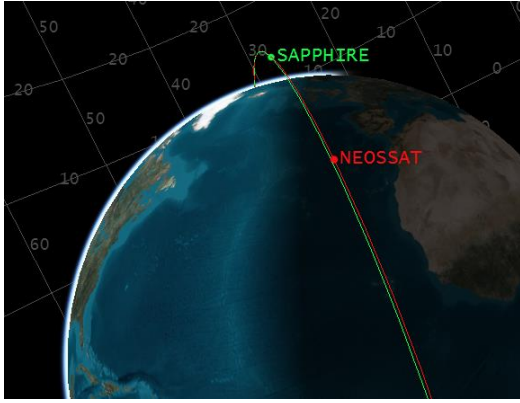
Figure 22 Relative orbit positions of NEOSSat and Sapphire 13 Jul 2018

Imagery was acquired in 2x2 binning for two 215 arcseconds/s slews, with durations of 5 and 12 minutes with Sapphire visible in most imagery acquired. The observations acquired were of sufficient metric accuracy to allow for orbit determination of Sapphire (Fig. 23), and orbital uncertainty was improved, with in-track uncertainty showing substantial improvement (Fig. 24).
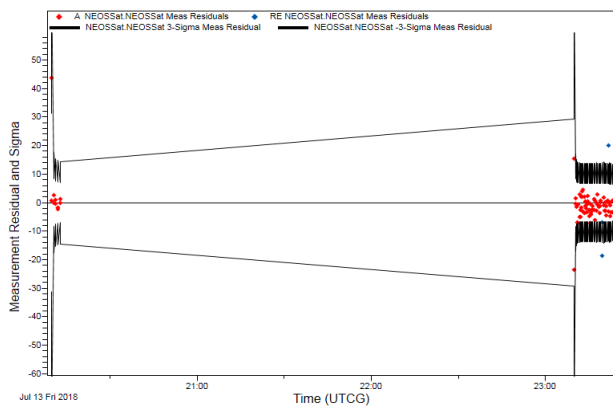

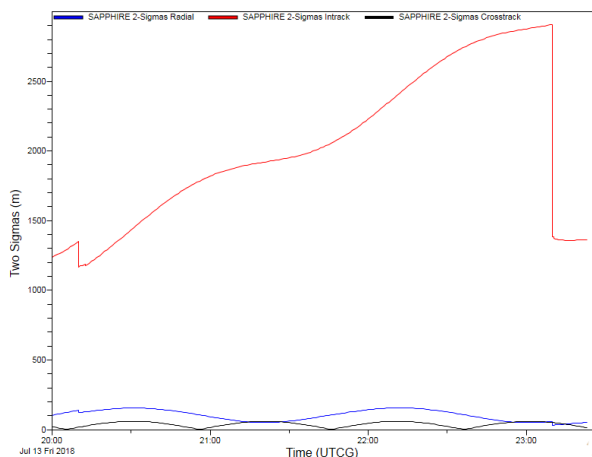*Figure 23 Kalman filter residuals from measurements of Sapphire observations in a lead-follow configuration*

Figure 24 Covariance improvement from Kalman filtered lead-follow observations

5.7. Proximity Observations

In June 2018, NEOSSat and Sapphire's orbital positions coincided, allowing for imagery to be taken at extremely close ranges (<50 km) during periods when Sapphire's relative angular rate fell within the NEOSSat's ACS tracking limit. The resulting images are shown in Fig. 25.

The proximity events with Sapphire occurred over six orbits on 12 Jun 2018, from 04:12:14 UTC to 12:41:55 UTC on the same day. Within these passes, NEOSSat was able to track and collect 55 observations.

As NEOSSat is designed for deep space observations, the very close proximity of Sapphire created significant blooming in the imagery. This had the effect of slightly downgrading the metric accuracy of the observations due to increased uncertainty in centroiding.
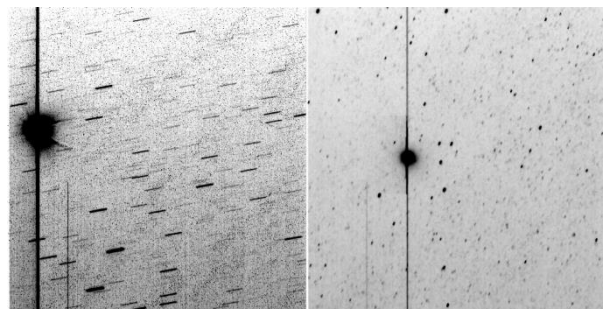

Figure 25 Close proximity images of Sapphire at 50 km (left) and 47 km (right)

The large difference in brightness between the two images in Fig. 25 is due to solar phase angle rather than range. Fig. 26 shows the relative positions of NEOSSat and Sapphire during one such encounter. The red trace in Fig. 26 shows the position of Sapphire relative to NEOSSat during one orbit.
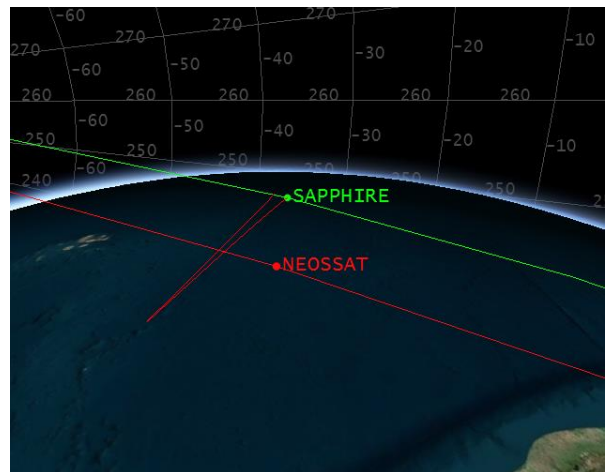

Figure 26 Relative orbit positions of NEOSSat and Sapphire at 12 June 2018 12:40:30 UTC

Fig. 27 shows the close ranges at which imaging occurred throughout the day.
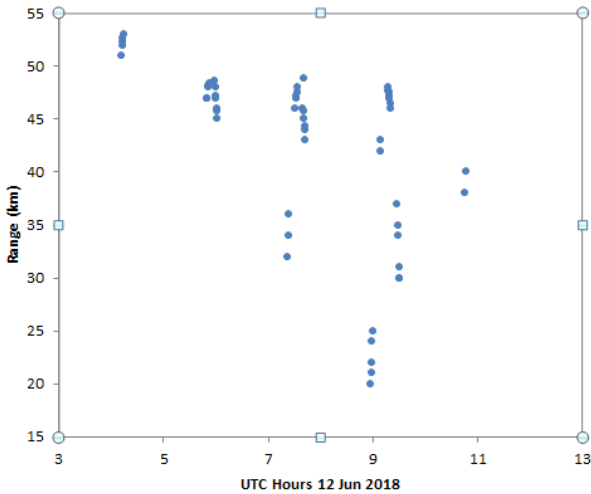
Figure 27 Range values for proximity observations of Sapphire

Interestingly, unlike most optical orbit determinations, it was the cross-track axis uncertainty (Fig. 28) which improved the least during Kalman filtering. Optical observations are normally done at high range and thus typically provide the least improvement in the radial component due to the angles only nature of the data.
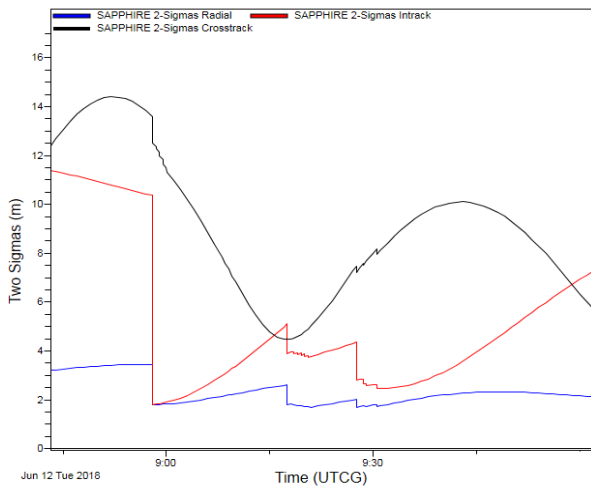

Figure 28 Position Uncertainty updates with close proximity observations

5.8. Future Directions

New SSA applications outside its deep space observation mission are now being explored with NEOSSat. We believe that we have characterized the first observations of fast-approaching objects during self-conjunction. LEO conjunction monitoring and persistent tracking of HVAs have also been demonstrated. Close proximity tracking demonstrations will enable proximity monitoring tests around Canadian satellites and could play a role in future on-orbit servicing. Proximity observations with slant ranges down to 20 km have been achieved and are being exploited for their astrometric and photometric value.

6. NEAR-EARTH OBJECT ASTROMETRY

For its NEO mission, a key advantage of NEOSSat is the ability to acquire astrometric observations at solar elongation as small as 45 degrees in routine operations, and, during the eclipse season, to within 15 degrees from the sun (Fig 29). This, combined with the ability to measure parallax (Fig. 30), has suggested that NEOSSat is an ideal sensor platform for those extreme cases of close Earth encounters that are becoming more and more frequent; not because there are more events but because the large surveys have become more efficient at finding smaller and more numerous objects.
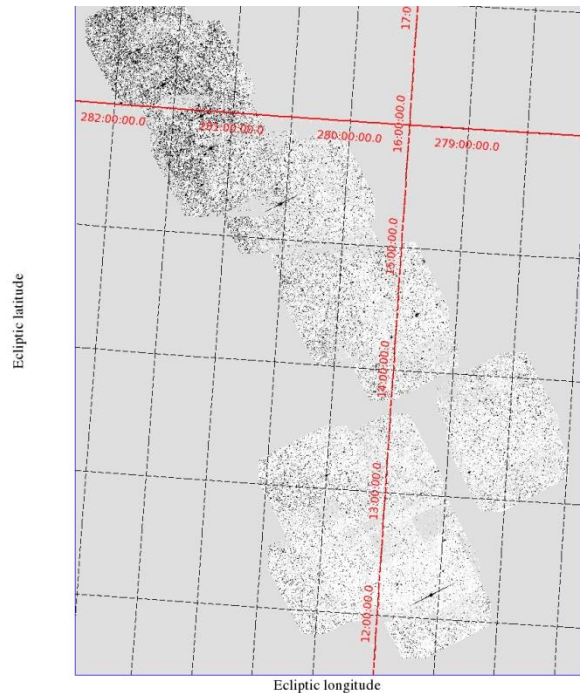

Figure 29 Field distribution of 213 low solar-elongation survey images, obtained over a 72-hour period (UT 2018 Dec. 22-24) and re-sampled onto an ecliptic (8^0 x 5^0) projection. The south-western field is 13.8^0 from the sun.

6.1 NEO Follow-Up with NEOSSat

In many cases, the survey instruments themselves serve to perform the astrometric follow-up work that is required for orbital calculation and risk assessment, however, when the object rapidly recedes to low solar elongation, it is necessary to employ other, more specialized sensors.

The most critical follow-up takes place within three days of discovery because the initial observations are usually insufficient to even broadly identify the orbital properties of the new object [15]. This is because a small number of observations by a single observatory over a short timespan does not contain enough information to determine the geocentric distance of the object - there is very little parallax information. As a result, ephemerides rapidly become extremely uncertain or useless.

One of the most difficult parts of Gauss's sector-triangle ratio method for the calculation of a set of preliminary orbital elements of an asteroid or comet involves successive iteration of the so-called 'triangle equations'. Primary among the unknowns is a set of geocentric radii vectors at three times that are generally found by iteration of a series. However, NEOSSat astrometric observations will, at the very least, have the ability to constrain these unknown distances.

6.2 Astrometric Reduction of NEOSSat Images

Using software tools adapted from a long-existing NEO studies program in Victoria [15] [16], a feasibility study was conducted to determine the usefulness of NEOSSat for rapid astrometric follow-up of newly-discovered NEO candidates. There are two advantages associated with an orbiting sensor such as NEOSSat: 1) it is possible to directly measure the parallax of a candidate (Fig 30) in a single orbit of the bus, and, 2) the sensor is not subjected to the usual problems encountered by ground-based sensors, i.e. the cycle of day and night and inclement weather conditions.
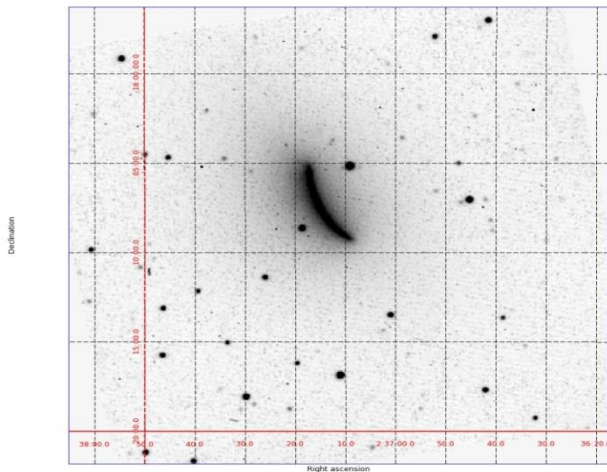

Figure 30 The effect of parallax upon a stack of 70 images, obtained through 1/3 of the orbital period of NEOSSat. The object is Periodic Comet Wirtanen (46P) as seen on UT 2018 Dec. 02 when the comet was 0.116 AU from the Earth. The geocentric motion vector was 261 arcseconds per hour at position angle 26.5 ^{0}.

The data reduction pipeline corrects for instrumental trends (bias and dark subtraction) and performs an astrometric calibration of each 0.8 degree field. In the first pass, the images are rotated closely to the celestial coordinate system, using the field rotation parameter in each image header and re-sampled onto a flat (tangential) frame. Source catalogues are generated of all point sources (stars) in the field, using Gaussian fitting, while one of a selection of astrometric catalogues are called (Tycho2, PPM, Carlsberg Meridian Circle, USNO and 2MASS) and predictions of the detector positions of each catalogue source are calculated using the first pass world

coordinate system (WCS) information in the image header. The two lists are then cross-correlated, the catalogue source positions are determined using Gaussian fitting and the final WCS is determined. All pixels are then re-sampled to the ICRS reference frame. An example of the final data product is seen in Fig 31.
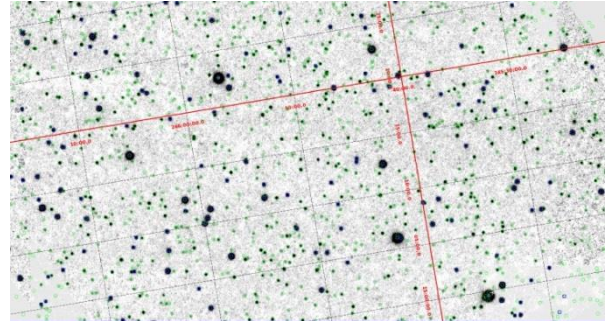

Figure 31 A section of a fully-calibrated NEOSSat image, resampled to the ICRS frame showing Tycho-2 catalogue stars (white cross), Carlsberg Meridian Circle catalogue (blue) and PPM catalogue stars (green). The coordinate grid is ecliptic J2000.

Given the relatively large field size of NEOSSat (0.8 degree), it is necessary to cull the lists of astrometric standard stars as a function of apparent magnitude. This is most acute at low galactic latitude where there may be thousands of faint standard stars. Astrometric solution residuals are in the range of 0.15-0.35 arcseconds RMS.

Astrometric observations from recent NEOSSat imaging runs have been submitted to the Minor Planet Center (MPC) and subsequently published in the Minor Planet Electronic Circulars, and the monthly Minor Planet Circulars of the International Astronomical Union.
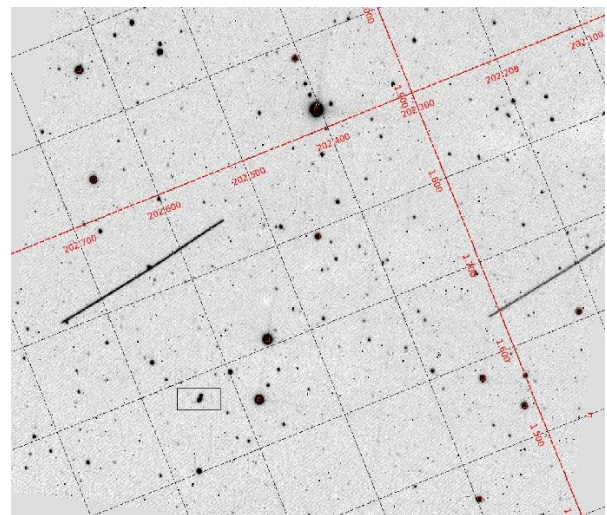

Figure 32 Near-Earth asteroid 2017-VR12 (boxed) seen on UT 2018 Mar. 07 at a distance of 0.010 AU and projected on ecliptic J2000 coordinate frame. Streaks are geostationary satellites imaged on the same frame. NEOSSat tracked 2017-VR12 closely at its Earth fly-by.

Spacecraft astrometry is unique as it yields not only angles-only data, but also a direct measure of parallax. For this reason, the new IAU-recognized format for spacecraft observations must also include the geocentric Cartesian coordinates of the bus. The traditional 80-column text format for astrometry is no longer the preferred format for submission of observations to the MPC. Instead, all observations (tracklets) are transmitted to the MPC and immediately proliferated to the Jet Propulsion Laboratory (Center for Near-Earth Object Studies) and the (European Space Agency) NEO Coordination Center, part of the Space Situational Awareness NEO segment (SSA-NEO), in the new Astrometric Data Exchange Standard (ADES) comprised of xml format files [17]. The ADES has been found to be much more comprehensive and observations are ingested in real time by all organizations.

6.3 Future Directions

An asteroid detection from a ground-based sensor on a single night is referred to as a "tracklet"; a set of two or more detections of the object aligned along a line or great circle. An example of a near-Earth asteroid tracklet observed by NEOSSat is seen in Fig. 33, where eleven short exposures have been aligned and co-added to reveal the objects curved trajectory through the star field. A tracklet from a ground-based sensor can be easily modelled as either linear or very slightly curved. The situation is complicated when the instrument is space-based; especially when the bus is in a high-inclination, low Earth orbit, such as NEOSSat, where the effects of parallax are significant and results in a highly non-linear motion pattern across the detector.
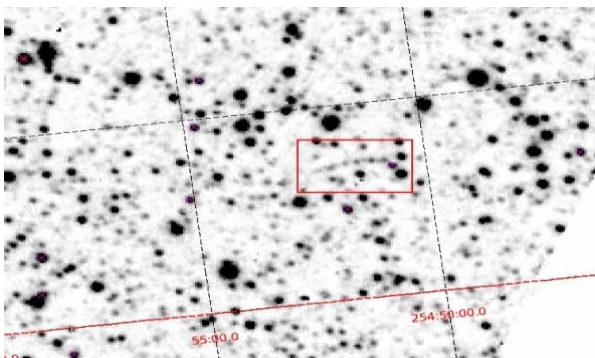

Figure 33. A stack of 11 NEOSSat images, co-added at sidereal rate showing the tracklet of near-Earth asteroid 2002 AJ129 on UT 2018 Feb. 03. The geocentric motion vector was 26 °/day at position angle 281 °

A limiting factor for the detection of faint and fast-moving objects is trailing loss on the detector. Once the target object has begun to trail beyond the "seeing disk" on the detector the effective exposure duration has ended and the astrometric accuracy has begun to degrade. Trailing loss can be negated by using the "shift&stack" technique. This is a straight-forward procedure for a

ground-based sensor, where a series of short exposure CCD images are obtained at the predicted position of a fast-moving NEO with the exposure time set by the objects plane-of-sky motion rate. The duration of each exposure in the stack corresponds to the time it takes for the object to subtend the 'seeing disk'. By co-adding a series of exposures, appropriately shifted to place all flux from the target object into a seeing disk we have created a long exposure image. An example of the technique is seen in Fig. 34 where 31 short exposures (19 seconds each) have been co-added to compensate for the motion of the NEO (2.3 degrees/day at position angle 102 degrees). Astrometry is usually performed on a second image that has been co-added with a median filter (see Fig 34, left frame). Since the only source that will be detected on the median-filtered image will need to match the predicted motion vector, we refer to this as a "keyhole" observation.

Figure 34. A shift&stack data set of a faint NEO. The stack consists of 31 exposures of 19 seconds duration obtained with the 1.82-m Plaskett telescope of the National Research Council of Canada. The 'seeing disk' for the night was 1.8"

Work is underway to develop a shift&stack routine for NEOSSat that will mimic the tracklet of an NEO, using knowledge of the heliocentric equatorial position of the Earth, the geocentric equatorial position of the spacecraft (NEOSSat) bus and a family of NEO preliminary orbits to generate a look-up table of heliocentric equatorial *radii vectores* of the NEO. The tracklet model should allow us to compensate for the non-linear motion of the NEO on the detector and place as much flux from the object as possible into a seeing disk.

7. CONCLUSIONS

7.1. Summary of Achievements & Innovations

In summary, overcoming some early mission challenges, NEOSSat has been able to advance the state-of-the-art in space-based surveillance of both NEO and RSOs. Some key achievements and innovations include:

- Track-rate imaging and metric observations of fast-moving LEO satellites/debris from a LEO platform at speeds up to 215 arcseconds/second

- Fine Point imaging of NEO survey fields and known asteroids/comets at low solar elongations, (under 15 degrees solar elongation during eclipse period)

The key drivers enabling the success of the NEOSSat mission include its innovative narrow-field star tracker enabling high-precision attitude determination and its precision reaction wheels with integrated rate sensors. Together with an attitude control system design that minimizes jitter and induced vibrations, the system achieves a high degree of pointing and tracking accuracy at arbitrary targets throughout the celestial sky from a relatively low-cost microsatellite platform.

NEOSSat's impressive performance at low solar elongations can also be attributed to the telescope's baffle, which successfully minimizes stray light from the Sun, Earth limb and Moon, enabling optical observations in regions generally inaccessible to ground telescopes.

7.2. NEO and RSO Surveillance Synergies

While the mission goals are different, there are several useful synergies between the NEO and RSO surveillance missions on NEOSSat. Both missions have benefited from NEOSSat's superior attitude control and baffle performance to image their targets at lower solar elongations than competing instruments. In addition, any developments done on image noise reduction, astrometric and photometric processing benefit both missions. While track-rate mode imaging operations were initially intended primarily for tracking fast-moving RSOs, they have been used routinely to track fast-moving asteroids as they make close approaches with the Earth. Similarly, the Fine Point operations intended primarily for the NEO survey operations have been used for imaging interesting RSO situations, such as close approaches, at key times. Shift&stack techniques for RSO tracklet detection and measurement are worth pursuing, as are star streak measurement techniques for NEO astrometry.

There are some areas where the requirements for RSO tracking and NEO survey differ. The NEO mission demands the best possible instrument focus to concentrate all the light from a faint target on a single pixel and maximize the achievable limiting magnitude. By contrast, the RSO surveillance mission benefits from a looser optical focus that spreads the same light over more pixels to provide sub-pixel accuracy on the metrics. Similarly, photometric applications benefit from slight de-focus to reduce the chances of pixel saturation and ensure that all light from a given object is measured.

7.3. Exoplanet Transit Photometry Application

Another exciting new development has been the recent utilization of NEOSSat for exoplanet transit photometry. The field of exoplanet astrophysics has seen an era of rapid discovery driven by thousands of confirmed planets discovered using photometric and spectroscopic techniques. Many transiting exoplanets were discovered with photometry from NASA's Kepler mission. Kepler exoplanet host stars have apparent visual magnitudes

typically fainter than V~12. The latest exoplanet mission, NASA's Transiting Exoplanet Survey Satellite (TESS), targets brighter stars (V~5-12). While Kepler was able to observe the systems for four years, the typical TESS target is limited to a few weeks of observations. Thus, additional observations are needed to better refine orbital periods and the photometric transit shape. Photometric observations from NEOSSat can contribute to this task.

To prepare for precision photometry, new image cleaning techniques for overscan, bias and dark correction were developed. The acquired overscan region is used to correct for electronic interference and bias offset. Using a Fourier series to model the coherent and repeating noise source, the amplitudes of detectable coherent noise range from 1 to 10 counts of Analog-Digital Unit (ADU). For dark correction, a master dark - a median average of all overscan and bias corrected darks that are relatively free of cosmic ray hits - is created based on acquired dark images from the same day as observations. The master dark is then scaled using a robust linear fit to match the science images. The master dark was found to scale extremely well with temperature.

Photometry was extracted using small apertures centered on stars of interest. Photometric centroids were estimated based on flux-weighted average. Background levels are locally estimated based on medians of pixels free of stars. For stars brighter than V~10, it was found that photometric uncertainties are photon-limited. Thus, noise from dark-current, electronic noise and stray light are not significant contributors. Observations of the WASP-33 exoplanet host star (Fig. 35) demonstrated a clear exoplanet transit detection and sub-milli-magnitude photometry based on short 1-second exposures. NEOSSat is currently collecting such follow-up light curves on a variety of TESS-detected transit candidates.
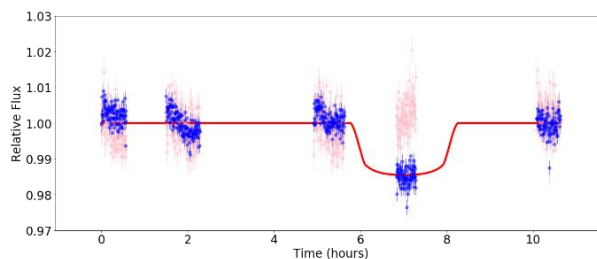

Figure 35. NEOSSat non-differential photometry with WASP-33 in blue, a nearby comparison star in pink, and the expected exoplanet transit model in red. The dip in flux is easily detected showing WASP-33b transit.

Five years after its launch, NEOSSat has become a unique platform to perform follow-up on candidate discoveries from other exoplanet hunting platforms. This work to develop advanced image cleaning techniques and precision photometry from NEOSSat will enable new possibilities for scientific investigations and characterization of RSO, NEO and other celestial objects.

7.4. Suggestions for Future Orbital Platforms

For future missions, the NEOSSat operations and science team would recommend active temperature control to ensure a consistent instrument performance independent of the telescope pointing. This would ensure that the natural dark current – itself a function of temperature – remains stable and well characterized.

Additional hardware redundancy would be beneficial to minimize impact of on-orbit hardware failures, such as those that crippled NEOSSat before flight software workarounds were developed. Nevertheless, now that this new software is part of platform's attitude control system baseline, a rebuild of NEOSSat would benefit from having three coarse attitude sensors (coarse sun sensor, magnetometer and GPS) and two options for desaturation (torque rods and dipole desaturation), providing a level of redundancy.

As NEOSSat has increased its on-orbit imaging for a variety of users, it would also benefit from enhancements for automated data processing feeding into an automated task planning loop to trigger new follow-up observations. Scenarios envisioned are to enable rapid follow-up on newly discovered NEOs or high priority RSO situations, such as orbital break-ups or detection of unusual behaviour. The team is currently investigating the possibilities in this area.

8. REFERENCES

1. Ticha, M., Honkova, M., Ticha, J. & Kocer, M., (2015). *Highlights of Astronomy,* Vol. 16, XXVIIIth IAU General Assembly, August 2012 T. Montmerle, ed.

2. Carroll, K., Hildebrand, A., Balam, D., & Matthews, J (2000). NESS: Using a Microsatellite to Search For and Track Satellites and Asteroids, *14th AIAA/USU Conference on Small Satellites,* Logan, Utah, 2000

3. Walker, G., Matthews, J., Kuschnig, R., Johnson, R., Rucinski, S., Pazder, J., Burley, G., Walker, A., Skaret, K., Zee, R., Grocott, S., Carroll, K., Sinclair, P., Sturgeon, D., & Harron, J., (2003). The MOST Asteroseismology Mission: Ultraprecise Photometry from Space, *Publications of the Astronomical Society of the Pacific*, Vol. 115, No. 811, July 2003

4. Wallace, B., Scott R., Sale M., Hildebrand A. & Cardinal R. (2014). The Near Earth Object Surveillance Satellite: Mission status and CCD evolution after 18 months on orbit. *Advanced Maui Optical & Space Surveillance (AMOS) Technologies Conference*, Maui, Hawaii, 2014.

5. Jedicke, R., Granvik, M., Micheli, M., Ryan, E., Spahr, T. & Yeomans, D. (2015). *Asteroids IV*, (Eds. P. Michel, F. DeMeo & W. Bottke), University of Arizona Press, Tucson, United States, pp795-813.

6. Thorsteinson S. & Scott R. (2018). NEOSSat Space Situational Awareness Case Study: GOES 16 Relocation Tracking, *Canadian Aeronautics and Space Institute (CASI) ASTRO Conference*, Quebec, Canada, May 2018.

7. Scott R. & Thorsteinson, S. (2018). Key Findings from the NEOSSat Space-Based SSA Microsatellite Mission. *Advanced Maui Optical & Space Surveillance (AMOS) Technologies Conference*, Maui, Hawaii, 2018.

8. Thorsteinson, S. (2017). Space Surveillance from A Microsatellite – Metric Observation Processing from NEOSSat, Masters Thesis, Royal Military College of Canada. https://espace.rmc.ca/handle/11264/1364

9. Abbasi, V., Jackson, N., Doyon, M., Wessels, R., Sekhavat, P., Cannata, M., Gillett, R., & Eagleson, S. (2018)., NEOSSat Recovery Following Magnetometer and Torque Rod Failure", *15th International Conference on Space Operations (SpaceOps 2018),* Marseilles, France, May 2018

10. Eagleson, S., Abbasi, V., Jackson, N., Scott, R., Thorsteinson, S. & Wessels, R. (2018). Single GPS Antenna Attitude Vector Pair – NEOSSat Recovery. *32nd AIAA/USU Conference on Small Satellites*, Logan, Utah, 2018

11. Open Government, http://open.canada.ca

12. Abbasi, V., Babiker, F., Doyon, M., & Golla, D. (2017). Close Encounters of an Advanced Kind: Lessons Learned and New Approaches in Collision Risk Assessment and Mitigation, *Proceedings of the 7th European Conference on Space Debris*, Darmstadt, Germany, 2017

13. SOCRATES, http://www.celestrak.com/SOCRATES/

14. Wright, J. (2013). Orbit Determination Tool Kit: Theory and Algorithms. Technical report, Analytical Graphics Inc. http://www.agi.com/resources/white-papers/orbit-determination-tool-kit-theory-and-algorithms

15. Tatum, J. B., Balam, D. D. & Aikman, G. C. L. (1994). Astrometric follow-up and recovery of near-Earth asteroids. *Planetary and Space Science,* **42**(8), pp 611-621.

16. Balam, D. D. & Tatum, J. B. (1997). The Climenhaga Observatory Near-Earth Space Surveillance Program 1995. *Journal of the Royal Astronomical Society of Canada* **91**, pp 28-31.

17. MPEC 2018-N52: *ADES SUBMISSIONS AND THE NEW PROCESSING PIPELINE* https://www.minorplanetcenter.net/mpec/K18/K18N52.html

---